Vol. 71: 33–45, 2016
doi: 10.3354/cr01425

CLIMATE RESEARCH
Clim Res

Published online November 14

Long-term Bering Sea environmental variability revealed by a centennial-length biochronology of Pacific ocean perch *Sebastes alutus*

Peter van der Sleen[1], Matthew P. Dzaugis[1], Christopher Gentry[2], Wayne P. Hall[1], Vicki Hamilton[3], Thomas E. Helser[4], Mary E. Matta[4], Christopher A. Underwood[5], Rachel Zuercher[6], Bryan A. Black[1,*]

[1]Marine Science Institute, University of Texas at Austin, Port Aransas, TX 78373, USA
[2]Department of Geosciences, Austin Peay State University, Clarksville, TN 37044, USA
[3]Institute for Marine and Antarctic Studies, University of Tasmania, Battery Point, TAS 7004, Australia
[4]Resource Ecology and Fisheries Management Division, Alaska Fisheries Science Center, National Marine Fisheries Service, NOAA, Seattle, WA 98115, USA
[5]Department of Geography, University of Wisconsin-Platteville, Platteville, WI 53818, USA
[6]Department of Ecology and Evolutionary Biology, University of California, Santa Cruz, CA 95060, USA

ABSTRACT: The productivity and functioning of Bering Sea marine ecosystems are tightly coupled to decadal-scale environmental variability, as exemplified by the profound changes in community composition that followed the 1976–1977 shift from a cool to a warm climate regime. Longer-term ecosystem dynamics, including the extent to which this regime shift was exceptional in the context of the past century, remain poorly described due to a lack of multi-decadal biological time series. To explore the impact of decadal regime shifts on higher trophic levels, we applied dendrochronology (tree-ring science) techniques to the otolith growth-increment widths of Pacific ocean perch *Sebastes alutus* (POP) collected from the continental slope of the eastern Bering Sea. After crossdating, 2 chronology development techniques were applied: (1) a regional curve standardization (RCS) approach designed to retain as much low-frequency variability as possible, and (2) an individual-detrending approach that maximized interannual synchrony among samples. Both chronologies spanned the years 1919–2006 and were significantly ($p < 0.001$) and positively correlated with sea surface temperature (March–December). The RCS chronology showed a transition from relatively slow to fast growth after 1976–1977. In both chronologies, the highest observed growth values immediately followed the regime shift, suggesting that this event had a critical and lasting impact on growth of POP. This growth pulse was, however, not shared by a previously published yellowfin sole *Limanda aspera* chronology (1969–2006) from the eastern Bering Sea shelf, indicating species- or site-specific responses. Ultimately, these chronologies provide a long-term perspective and underscore the susceptibility of fish growth to extreme low-frequency events.

KEY WORDS: Otolith · Chronology · Growth increment · Bering Sea · Climate · Pacific ocean perch · *Sebastes alutus*

1. INTRODUCTION

The eastern Bering Sea supports some of the most economically valuable fisheries in North America as well as large populations of marine birds and mammals of conservation concern. The functioning of this ecosystem is tightly linked to environmental variability (e.g. Walsh & McRoy 1986, Hunt et al. 2002, 2011), which is especially pronounced on sub-decadal to multidecadal timescales. One of the best documented examples of these linkages is the 1976–1977 shift from relatively cool to warm ocean conditions (Hare

*Corresponding author: bryan.black@utexas.edu

& Mantua 2000), which resulted in marked community reorganization characterized by increases in biomass of walleye pollock *Gadus chalcogrammus*, Pacific cod *G. macrocephalus*, rock soles *Lepidopsetta* spp., flathead sole *Hippoglossoides elassodon*, and cartilaginous fishes (e.g. Hare & Francis 1995, Hollowed & Wooster 1995, Anderson & Piatt 1999, Hare & Mantua 2000, Conners et al. 2002). However, ecosystem variability on longer timescales remains largely undescribed due to a lack of multidecadal biological time series (Poloczanska et al. 2013, Litzow et al. 2014, Pörtner et al. 2014). A deeper historical perspective could help quantify the extent to which recent variability is exceptional in the 20th century context, and help benchmark impacts of climate change in a region that has some of the highest rates of anthropogenic warming in the world (Stabeno et al. 2012, Wang et al. 2012, Pörtner et al. 2014).

One approach to deriving long-term biological indicators is applying techniques developed for tree-ring research (dendrochronology) to growth-increment widths in fish otoliths (Black et al. 2005, 2014, Black 2009, Matta et al. 2010, 2016). Resulting chronologies can provide continuous, annually resolved (one value per year) and exactly dated growth histories that can be readily integrated with instrumental climate data or observational biological records. To date, growth-increment chronologies have been developed for 3 flatfish species from the Bering Sea, all of which strongly and positively relate to temperature, the longest of which is generated from yellowfin sole *Limanda aspera* (YFS) and dates back to 1969 (Matta et al. 2010, 2016, Black et al. 2013). Here, we utilize archival otoliths of Pacific ocean perch *Sebastes alutus* (POP hereafter) to develop a much longer, centennial-length growth chronology for the Bering Sea. Our specific goals were to: (1) evaluate climate drivers of POP growth; (2) quantify low-frequency variability including long-term trends; (3) provide context for evaluating late-20th-century environmental variability; and (4) evaluate synchrony between the Bering Sea continental slope and shelf by comparing POP with the existing YFS chronology.

2. MATERIALS AND METHODS

2.1. Sample preparation and measurement

POP are widely distributed over the outer continental shelf and upper continental slope of the North Pacific Ocean, ranging from Japan through the Bering Sea and Gulf of Alaska to southern California. Adult POP are generally found at 150–420 m depth, rising off the bottom at night to feed on euphausiids, mysids, amphipods, and midwater fishes (Leaman 2002). In the fall, females migrate farther offshore into deeper water (500–700 m), and return to shallower summertime habitats by late spring (Leaman 2002). The maximum reported age is 105 yr (Goetz et al. 2012) and the annual periodicity of increment formation has been confirmed via bomb radiocarbon analysis (Kastelle et al. 2008). POP otoliths were collected in the eastern Bering Sea in 1981, 2008, and 2010 during scientific bottom trawl surveys conducted by the National Marine Fisheries Service of the National Oceanic and Atmospheric Administration (NOAA); the 1981 sampling was part of a cooperative effort between the United States and Japan. The sampling area spanned approximately 50–61° N, 165–176° W along the continental shelf–slope break (Fig. 1A). While exact sampling locations were known for all otoliths collected in 2008 and 2010, latitude and longitude were not explicitly recorded for otoliths collected in 1981. However, the number of fish captured at each station was recorded during the survey, with 95% of the catch located in approximately the same area as those samples collected in 2008 and 2010 (Fig. 1A).

For this study, 100 otoliths (one per fish) were initially prepared. Otoliths were embedded in polyester resin blocks and thin-sectioned transversely through the core using a Buehler IsoMet linear precision saw (Buehler). Thin sections were mounted on glass slides and polished to a thickness of approximately 0.4 mm using wet and dry abrasive paper followed by 0.05 µm Buehler MasterPrep polishing suspension. Samples were imaged with transmitted light at either 100× or 200× magnification using a Leica MZ binocular microscope attached to a Leica DFC digital camera. Samples were chosen for crossdating and measurement if they were at least 40 yr old and had increments of sufficient clarity that boundaries could be well delineated. Of all the individuals ≥40 yr (50 samples), 50% met this clarity criterion (25 samples). Each annual growth increment consisted of one opaque and one translucent growth zone, which appeared as dark and light bands, respectively, when viewed with transmitted light (Fig. 1B).

We used crossdating to ensure that all increments were assigned to the correct calendar year of formation. This technique relies on the premise that some aspect of the environment influences annual growth and varies over time to induce a synchronous pattern in growth-increment widths across individuals of a given species and location (Douglass 1936, Fritts

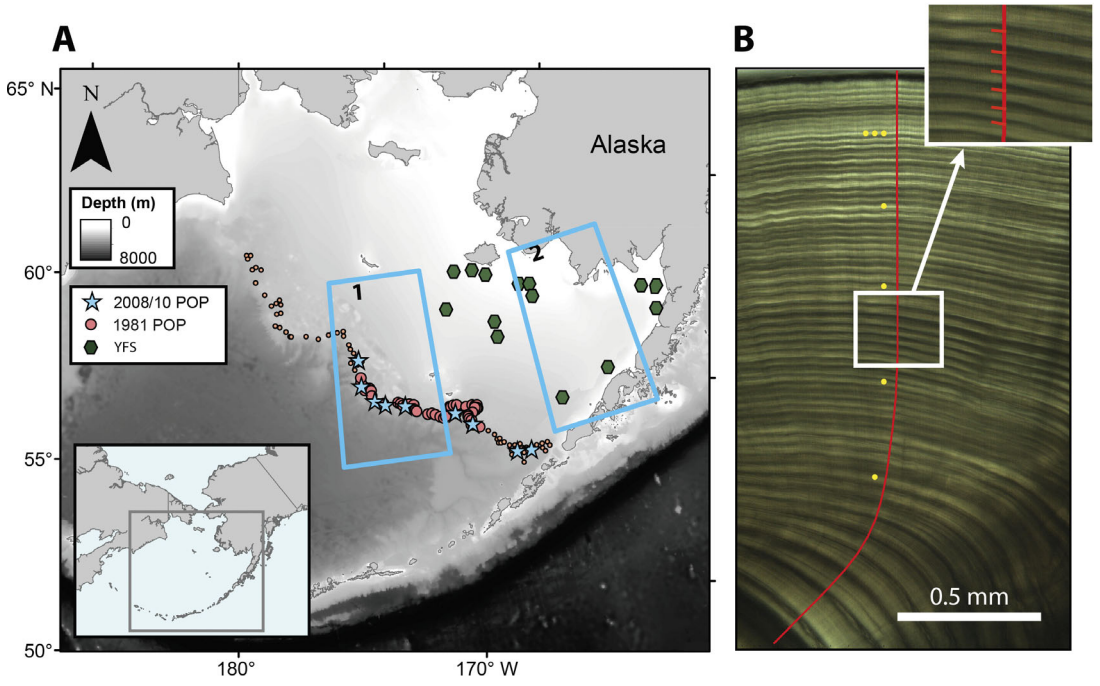

Fig. 1. (A) Sampling locations of Pacific ocean perch *Sebastes alutus* (POP) in the eastern Bering Sea. Blue stars indicate sampling locations for otoliths collected in 2008 and 2010. Red circles indicate hauls in which fish were caught during the 1981 trawl survey, with larger circles indicating regions over which 95% of all 1981 fish were caught. Green polygons indicate collection sites of yellowfin sole *Limanda aspera* (YFS). The blue rectangles indicate the 2 regions in which monthly sea surface temperature (SST) data were averaged and related to the POP and YFS chronologies (Region 1 = 55–60° N, 170–175° W; Region 2 = 55–60° N, 160–165° W). (B) Transverse section of a POP otolith imaged at 200× magnification and viewed with transmitted light. Increment width was measured along the axis of growth indicated by the red line; yellow dots indicate decades (3 dots represent the year 2000). The inset shows annual growth-increment boundaries delineated with red tick marks

1976). Increments that were anomalously wide or narrow were useful in the crossdating process, as were some rapid and sustained decadal-scale shifts in growth that were often accompanied by synchronous variations in otolith coloration (Black et al. 2005, 2008). These synchronous growth patterns were visually compared among individuals beginning at the marginal growth increment formed in the known year of capture, and working back toward the otolith core. If an increment was accidentally missed or falsely added, the growth pattern in that individual would be offset by a year relative to the other individuals in the sample set, indicating that a possible error had occurred. However, a dating correction was only made if the error could be confirmed by carefully re-inspecting the otolith structure for a missed increment, false increment, or other aberration.

Once all samples were visually crossdated, increment widths were measured continuously along the axis of growth and thus perpendicular to each annual increment boundary (Fig. 1B) using Image-Pro Premier v.9.1 (Media Cybernetics). Increments were measured from the distal boundary of the previous year's translucent zone to the distal boundary of the current year's translucent zone. The first 5 to 7 increments were excluded due to difficulties in delineating juvenile growth-increment boundaries. The increment at the otolith margin was also not measured because it was only partially formed. All otoliths were crossdated and measured along 3 to 4 different axes, resulting in multiple measurement series per fish. All axes were located on the proximal half of the otolith near the sulcal groove, a region in which increment boundaries were consistently parallel and clearly defined. Prior to all analyses, these series were averaged per fish to avoid issues of pseudoreplication.

2.2. Chronology development

Crossdating accuracy was statistically verified using the program COFECHA (Holmes 1983, Grissino-Mayer 2001). In COFECHA, each measurement time series was fit with a cubic smoothing spline set at a 50% frequency response of 22 yr, a value used for other rockfish species (Black et al. 2005). Observed increment width values were divided by those predicted by the splines, thereby isolating high-frequency variability and standardizing each meas-

urement time series to a mean of 1. Each standardized time series was correlated with the average of all others, the mean of which was reported as the inter-series correlation. In the event of a poor correlation ($p > 0.01$), the sample was visually re-examined, but measurements were not changed without clear evidence of an error. Mean sensitivity, an index of high-frequency (year-to-year) variability based on the difference in width between pairs of adjacent growth increments, was also calculated using COFECHA. Mean sensitivity can range in value from a minimum of 0 (a pair of increments of the same width) to a maximum of 2 (a pair in which one width is 0; Fritts 1976). Inter-series correlation and mean sensitivity are commonly reported in tree-ring analyses as measures of site-wide signal strength and growth variability, respectively, and are provided here to facilitate comparisons with other published chronologies.

Once crossdating was verified, the growth-increment width measurement time series were used to generate a chronology. Growth increments were grouped according to fish age at the time of increment formation, mean increment width was then calculated for each age group, and a negative exponential function was fit through these means (Fig. 2). Observed increment widths were divided by those predicted by the negative exponential function, thereby removing the age-related growth trend. The resulting standardized growth-increment values were averaged with respect to calendar year to yield the chronology and associated confidence intervals. This approach is similar to the regional curve standardization (RCS) approach applied to retain low-frequency variability in tree-ring datasets (Esper et al. 2002, 2003), and will hereafter be referred to as the RCS chronology.

In addition to RCS, we applied a second and more classical approach to chronology development, in which a negative exponential function was fitted through each otolith measurement time series, and observed increment widths were divided by those predicted. Standardized growth-increment values were averaged with respect to calendar year of formation to yield the chronology. We will refer to this chronology as the ID (individual detrending) chronology. The main disadvantage of this approach was that any low-frequency variability that exceeded the mean measurement time series length (50 yr) would be removed (the 'segment length curse'; Cook et al. 1995). The advantage, however, was that any differences in growth rate due to geography would be removed and would not impact the outcome of the chronology. Moreover, the RCS chronologies tended to have higher levels of uncertainty, especially with smaller sample numbers. Thus, the combination of

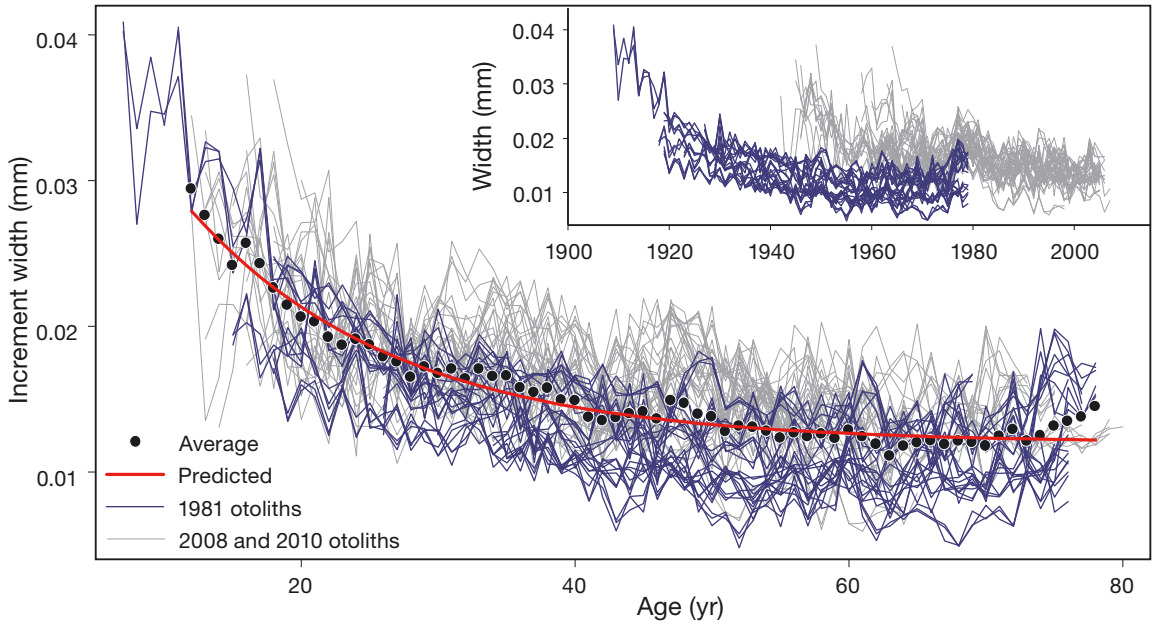

Fig. 2. Otolith measurement time series for Pacific ocean perch *Sebastes alutus* (POP), arranged by calendar year (inset) and fish age at time of increment formation. Dataset contains otoliths collected in 1981 (blue lines), and 2008 and 2010 (gray lines). The POP chronology was generated by calculating the average increment width for each age (black dots) and fitting those means with a negative exponential function (red line). The observed increment widths (blue and gray lines) were subsequently divided by the predicted (red line) width to remove age-related growth trends. The mean of these detrended series is the regional curve standardization (RCS) chronology

the ID and RCS approaches provided complementary perspectives of POP growth in the Bering Sea.

For both chronologies, the expressed population signal (EPS) was calculated in running 30 yr windows to quantify how well the chronology represents the theoretical population from which the fish were sampled (Wigley et al. 1984). Albeit arbitrary, an EPS ≥ 0.85 is often used as a threshold at which the common signal is considered sufficiently strong for climate reconstruction, and served here as an index of the strength of the synchronous, population-wide growth pattern relative to individual-level variability (Wigley et al. 1984, Briffa & Jones 1990). To better assess low-frequency variability, mean increment-width index and associated 95% confidence intervals were calculated in non-overlapping 10 yr windows along the length of each chronology. This analysis was performed across all detrended individuals (often ≥100 values) as opposed to using the master chronology values. We also used regime-shift detection software (SRSD, v.6) based on a STARS sequential *t*-test analysis (Rodionov 2004, 2006) to examine the chronology for any significant ($p < 0.01$) step changes (regime shifts) ≥20 yr in length. Regime shift detection was halted 10 yr prior to the end of the chronology to avoid edge effects. A 'tuning constant' was applied to reduce the effects of outliers >2 SD outside the distribution of chronology values (Rodionov 2004, 2006). Given that the POP chronologies exhibited considerable autocorrelation, the significance level was penalized by adjusting downward the degrees of freedom in the regime-detection analysis (Rodionov 2006).

Although 95% of the 1981 otoliths were sampled in a region that closely overlapped with the 2008 and 2010 otoliths, there exists the unlikely possibility that some specimens used in the chronology came from farther north (Fig. 1A). If growth rates were inherently lower at these higher latitudes, combining the 1981 samples with the 2008 and 2010 samples could give the illusion of an increase in increment width in the chronology around 1981. In other words, we would not be able to disentangle whether a sustained change in growth rate was due to a regime shift (circa 1977) or that the fish collected in 1981 lived in a different region with its own unique environmental conditions and growth rates. However, the effects of latitude on growth could be at least partially addressed using the 2008 and 2010 samples. Increment width and age of formation were log-transformed, which linearized each measurement time series. Each transformed measurement time series was fitted with a linear regression (of increment width against age), and the slopes and intercepts of those regressions were plotted with respect to latitude of collection. Any relationship between latitude of collection and slope or intercept could indicate a significant geographic gradient, at least over the region from which the 2008 and 2010 samples were obtained.

2.3. Climate–growth relationships

Temperature data were obtained from 2 sources: monthly sea surface temperature (SST; 1970–2006) at oceanographic mooring 2 (57° N, 164° W; available at www.beringclimate.noaa.gov/data/index.php), and 1° gridded monthly Hadley SST (Hadley ISST1; Rayner et al. 2003). Monthly gridded sea-ice concentration data for the region were obtained from the National Snow and Ice Data Center (NSIDC; Cavalieri et al. 1996, data available since 1978). Monthly temperature and sea-ice concentration values, averaged over the region 55°–60° N, 170°–175° W, were correlated to the POP chronology. For both Hadley ISST and NSIDC sea-ice concentration, months with significant relationships ($p < 0.01$) were averaged, and a correlation map for that window of months was generated using the KNMI Climate Explorer (Trouet & Van Oldenborgh 2013). A stepwise multiple regression (threshold for inclusion: $p < 0.05$) was performed to identify the amount of variance in the chronology that could be explained by these regional climate variables. Given high levels of autocorrelation in the POP chronology, the 1 yr lag (i.e. the increment value of the previous year) of the chronology was also included as a predictor. Finally, the chronology was correlated to monthly averaged values of the multivariate El Niño-Southern Oscillation index (MEI; Wolter & Timlin 2011) and Pacific Decadal Oscillation index (PDO; Mantua et al. 1997).

We also built a chronology using only the 1981 samples and compared this with Hadley ISST 1° gridded SST and then repeated this process using only the 2008 and 2010 otoliths. The degree of spatial overlap between the correlation fields of the 1981 samples and the 2008 and 2010 samples was used to corroborate the provenance of the 1981 otoliths.

2.4. Relationships to other Bering Sea chronologies

Five flatfish otolith chronologies have been developed for the eastern Bering Sea, the longest of which, YFS (1969–2006), overlaps nearly 40 yr with our POP chronology (Matta et al. 2010, 2016, Black et al. 2013). The same RCS approach was used in its development

(Black et al. 2013). For comparison with POP climate–growth relationships, the YFS chronology was also compared with monthly means of 1° Hadley ISST data averaged over the region of sample collection (Fig. 1A). Those months that significantly ($p < 0.01$) correlated to the chronology were averaged, and a correlation map was generated using the KNMI Climate Explorer (Trouet & Van Oldenborgh 2013).

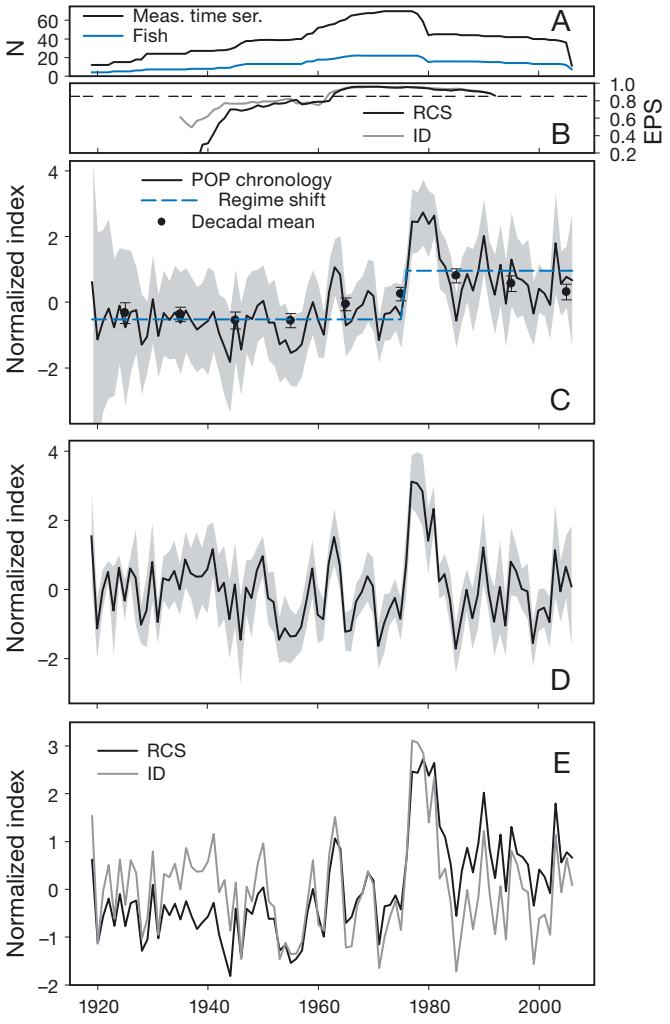

Fig. 3. Pacific ocean perch *Sebastes alutus* (POP) regional curve standardization (RCS) and individual-detrending (ID) chronologies and their properties. (A) Sample depth (number of measurement time series contributing to the chronology). (B) Expressed population signal (EPS, as calculated from the number of fish, not the number of measurement time series) and the 0.85 'ideal' threshold (dashed line). (C) POP chronology resulting from the RCS detrending approach; gray shading represents 95% confidence intervals for the annual values, the dots are decadal means, error bars show the 95% confidence intervals of the decadal means, and the blue dashed line shows the regime shift. (D) POP chronology resulting from the ID approach. No regime shift was detected in this chronology. (E) The 2 POP chronologies

3 RESULTS

3.21. POP chronologies

Of the 100 original samples initially prepared for this study, otoliths from 16 fish collected in 2008 and 2010 and 9 fish collected in 1981 had increments of sufficient clarity to provide continuous measurements over multiple decades (30–71 yr). Out of these 25 fish, 7 were female, and there was no indication that sex was a relevant factor for chronology development. All samples with visible increments had synchronous growth patterns and could be crossdated regardless of sex. All 72 measurement time series (from 25 fish) contained exponential growth declines, and otoliths collected in 1981 tended to grow more slowly than those collected in 2008 and 2010 (Fig. 2). Inter-series correlation was 0.44 while mean sensitivity was 0.14.

The 2 detrending techniques yielded somewhat different outcomes (Fig. 3). Most notably, the RCS approach captured a clear regime shift for which growth rates were significantly ($p < 0.001$) higher after 1976–1977 (Fig. 3C). The significance of this shift was insensitive to the value of the tuning constant or method of accounting for autocorrelation in the regime-shift detection software. A lower growth rate prior to 1976–1977 was also evident in decadal means, which were consistently lower prior to 1976–1977 than those values that followed (Fig. 3C). This 'step' in growth at the 1976–1977 shift was not evident in the ID chronology (Fig. 3D,E). Both chronologies, however, captured a profound growth pulse that followed the 1976–1977 shift, characterized by values that exceeded any others in the century-length record (Fig. 3). Confidence intervals were overall much narrower in the ID chronology, especially early in the record, and EPS values were comparatively higher (Fig. 3).

3.2. Climate–growth relationships

Climate–growth relationships were very similar for the RCS and ID chronologies, but the RCS chronology more clearly captured low-frequency variability; therefore, only results for the RCS chronology are presented. The POP chronology significantly ($p < 0.05$) correlated with SSTs at oceanographic mooring 2 (1970–2006) for all months except January. Strongest correlations were found with SST in the months April to August ($p < 0.001$; results not shown). When considering 1° gridded Hadley ISST data, we

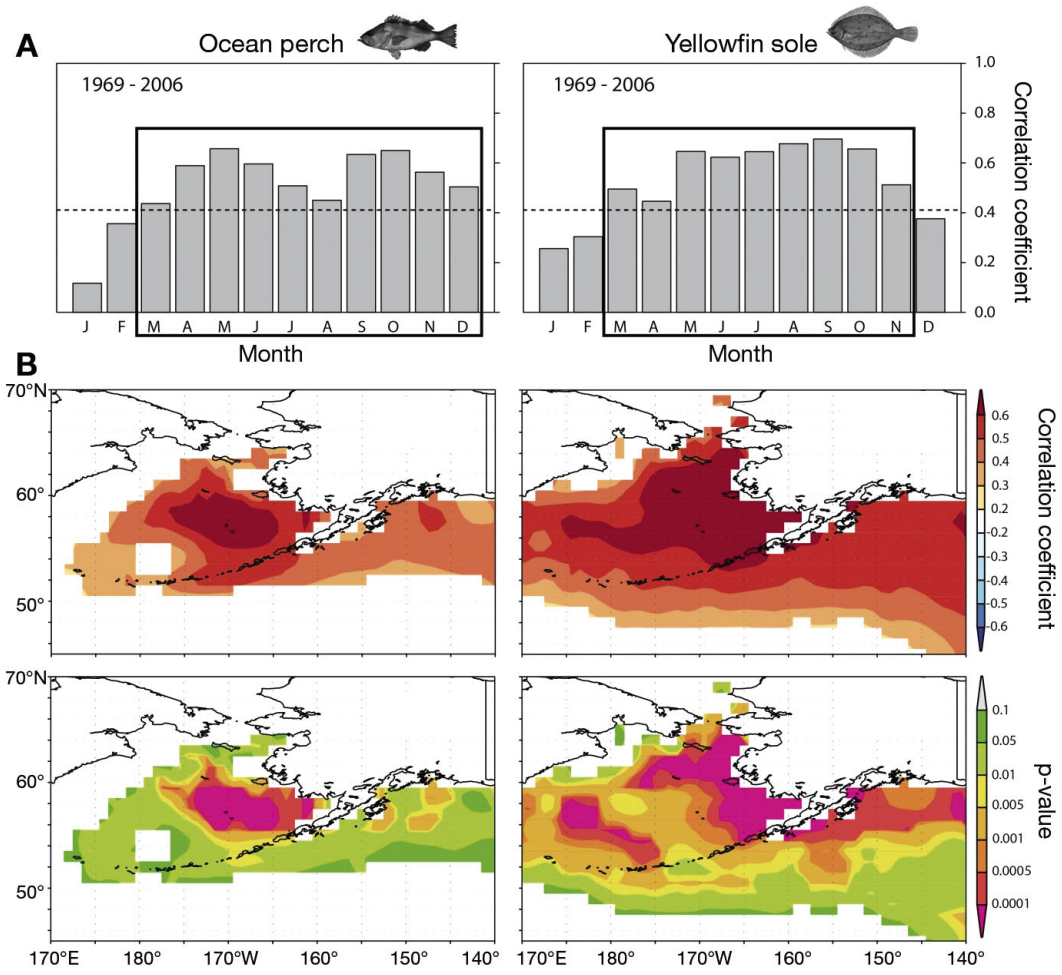

Fig. 4. Correlations of Pacific ocean perch *Sebastes alutus* (POP) regional curve standardization (RCS) (left panels) and yellowfin sole *Limanda aspera* (YFS) (right panels) chronologies with sea surface temperature (SST) data (Hadley ISST1). (A) Correlation coefficients of the POP and YFS chronologies with monthly-averaged SST (1969–2006) in Region 1 and Region 2, respectively (see region boundaries in Fig. 1A). Dashed line indicates significance level of $p < 0.01$. The rectangle indicates the months across which SST was averaged to generate correlation maps. (B) Correlation coefficients and p-values for the relationship between each chronology (1969–2006) and gridded SST

initially focused on the 1969–2006 interval, as this is the timespan shared with the YFS chronology and should also represent a period over which observed SST records are relatively dense (Matta et al. 2010). Region 1 (Fig. 1A) SST significantly ($p < 0.01$) and positively correlated with this truncated POP chronology in all months except January and February (Fig. 4A). However, results were similar for the full POP chronology (1919–2006), which significantly ($p < 0.01$) and positively correlated with SST in all months except January (Fig. S1 in the Supplement at www.int-res.com/articles/suppl/c071p033_supp.pdf). After averaging across the March to December window, correlations (1969–2006) with gridded SST were significant over a broad region of the shelf break that corresponded with sample provenance (Fig. 4B). The correlation pattern was similar in extent but weaker in strength when calculated over the full 1919–2006 interval (Fig. S1 in the Supplement). Monthly NSIDC ice concentration in region 1 (1979–2006) did not significantly correlate with the POP chronology (Fig. S2 in the Supplement, although correlation coefficients were strongest for April ($r = -0.35$, $p = 0.07$) and May ($r = -0.34$, $p = 0.07$). After averaging April and May gridded sea-ice concentration and comparing the POP chronology with the full field of available data, much stronger correlations were identified in the northeastern part of the Bering Sea (Fig. S2 in the Supplement).

With respect to indices of teleconnected climate phenomena, a significant positive correlation was found between the POP chronology and PDO index for all months ($p < 0.05$) except January, June, November, and December, as well as with average

annual PDO index (r = 0.293, p = 0.006) over the period 1919–2006 (Fig. S3 in the Supplement). A significant correlation was also found between the POP chronology and the average annual MEI (r = 0.409, p = 0.002) and monthly mean MEI (p < 0.01 for every month) over the period 1950–2006 (MEI data available since 1950; Fig. S3 in the Supplement).

3.3. Latitudinal effects

For the chronology generated using only the 1981 POP samples, correlations with gridded SST largely overlapped that of the full sample set and of a chronology generated with only the 2008 and 2010 samples (Fig. S4 in the Supplement). This corroborates that the 1981 samples spatially overlapped with the 2008 and 2010 samples. In addition, the slope and intercept (as proxies for growth rates) of log-transformed 2008 and 2010 measurement time series did not significantly relate to latitude of collection (p = 0.470 and p = 0.888, respectively). Only 11 of the 2008 and 2010 individuals shared a common interval of >30 yr (common period used: 1970–2006) and could be used in this analysis. However, latitude was not significantly related to growth rates, at least in the region from which the 2008 and 2010 samples were collected.

3.4. Relationships with the YFS Bering Sea chronology

The POP chronologies significantly correlated with the YFS chronology over the common 1969–2006 interval, illustrating at least some degree of synchrony across species and locations (Fig. 5). Perhaps the most conspicuous difference between the chronologies was that YFS did not share the profound growth pulse following the 1976–1977 regime shift (Fig. 5). Although YFS did experience a growth anomaly around 1977, a large growth pulse also occurred in the early 2000s, rising sharply from an anomalously low value in 1999 (Fig. 5). The YFS chronology also significantly and positively correlated with gridded SST, especially in the region from which specimens were collected on the southeastern Bering Sea shelf (Fig. 4B).

Another major difference between the POP chronology and the YFS chronology was that POP had a high level of first-order autocorrelation (correlation coefficient = 0.608) over the period 1969–2006, whereas no significant first-order autocorrelation was detected in the YFS chronology (coefficient = 0.157). In a multiple stepwise regression, the 1 yr-lagged chronology (13%) and SST (42%) together explained 55% of POP chronology variance (Table 1). For YFS, the 1 yr-lagged chronology was not significant (Table 1), while SST (29%) and sea-ice concentration (28%) together explained 58% of chronology variance (Table 1).

4. DISCUSSION

4.1. Chronology development

Half of the otoliths >40 yr in age (25 out of 50) were excluded from measurement due to difficulties in clearly identifying annual increment boundaries. This selection, being a consequence of the dendrochronological approach used here, could create a bias if the samples excluded (i.e. those with unclear increments) grew consistently differently, or responded fundamentally differently to climate variability, in comparison to the samples included (i.e. those with clear increments).

The longevity of POP combined with access to otoliths collected in 1981 allowed us to produce an exactly dated growth history that represents the longest annually resolved biological time series available for the Bering Sea, and to our knowledge, the longest cross-dated fish chronology yet developed anywhere in the world (spanning 1919–2006). There

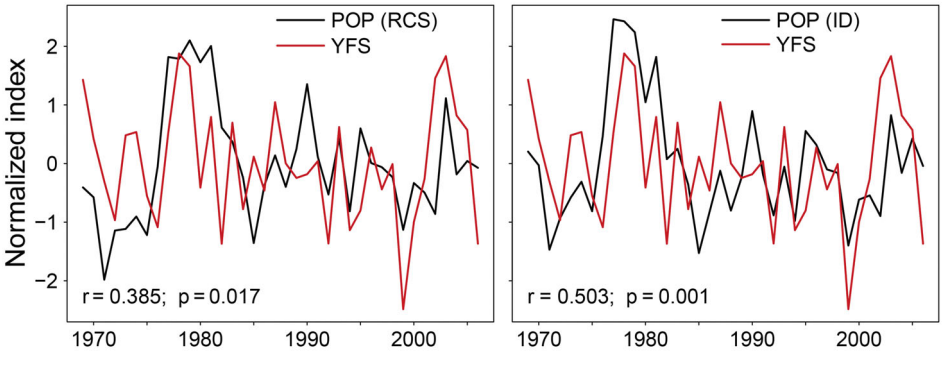

Fig. 5. Yellowfin sole *Limanda aspera* (YFS) chronology from the eastern Bering Sea (Matta et al. 2010) with the Pacific ocean perch *Sebastes alutus* (POP) regional curve standardization (RCS) chronology (left panel) and the individual-detrending (ID) chronology (right panel). Shown are the correlation coefficient and associated p-value

Table 1. Multiple regression analyses with 3 factors: sea surface temperature (SST), sea-ice concentration, and previous-year growth value. The time period analyzed for Pacific ocean perch *Sebastes alutus* (POP) was 1969–2006, and for yellowfin sole *Limanda aspera* (YFS) was 1978–2006 (due to the absence of sea-ice data prior to 1978). SST (shelf) refers to the average SST (April–December) in Region 1 in Fig. 1A; SST (shore) refers to average SST (March–November) in Region 2 of Fig. 1A; POP(t – 1) refers to the previous-year value in the POP chronology; Sea ice con. refers to average sea-ice concentration in March–April–May in Region 2

POP		$R^2_{adjusted}$ = 0.555			YFS		$R^2_{adjusted}$ = 0.586		
	Estimate	SE	t	p		Estimate	SE	t	p
Intercept	0.0950	0.1442	0.659	0.5145	Intercept	0.0269	0.2322	0.116	0.909
SST (shelf)	0.0939	0.0204	4.605	<0.0001	SST (shore)	0.1649	0.0366	4.511	0.0001
POP(t – 1)	0.4495	0.1309	3.435	0.0015	Sea ice con.	–0.9194	0.3536	–2.600	0.015

was a clearly synchronous growth pattern shared among individuals, though the POP inter-series correlation of 0.44 was relatively low compared with values of approximately 0.55 found in many other Pacific *Sebastes* spp. chronologies (Black 2009). The average length of individual time series was comparable to other studies (around 50 yr), as was the spatial extent over which samples were collected. For example, *Sebastes diploproa* and *S. ruberrimus* were collected over approximately 3 to 4 degrees latitude in the north-central California Current (Black 2009). Different in POP was the relatively poor delineation of growth-increment boundaries and the relatively low degree of interannual variability in width (i.e. 'complacent'). Farther south in the California Current, El Niño events periodically induce highly visible timestamps in the form of profoundly narrow growth increments that greatly facilitate crossdating (Black et al. 2014). Although interannual variability was sufficient for crossdating, Bering Sea POP generally lacked such conspicuous year-specific markers. Even during the initial visual assessment of the samples, decadal-scale environmental processes, and especially the 1976–1977 regime shift, dominated growth variability in this sample set.

The 2 methods of chronology development yielded somewhat different perspectives of POP growth history (Fig. 3). The greatest difference was that the RCS approach preserved differences in overall growth rate between the 1981 samples and the 2008 and 2010 samples, thereby capturing the sustained growth increase that followed the 1976–1977 regime shift. Such information was lost when each measurement time series was fit with a unique negative exponential function. A drawback of the RCS approach, however, was that it added considerable uncertainty around estimates of mean growth, especially in calendar years when sample numbers were low. This effect has also been reported in tree-ring datasets to which this technique has been applied (e.g. Esper et al. 2002, 2003). However, long-term trends in the POP growth index could still be quantified by examining the decadal growth rate or applying STARS algorithms, which corroborated the importance of the 1976–1977 regime shift. Moreover, the ID chronology also captured the profound growth pulse that followed the regime shift, and rapid growth was evident in fish of all ages and collection sources, appearing as a series of conspicuously wide increments.

A potential complication with the POP chronologies was that the exact sampling locations of the 1981 otoliths were unknown. The vast majority of 1981 sampling overlapped with that during 2008 and 2010, but there is the unlikely possibility that some 1981 samples originated from much farther north (Fig. 1A). This would be an issue if northern otoliths grew inherently slower than those in the central study region. Under such a scenario, pre- and post-regime shift differences in the RCS chronology could be an artifact of different growth rates between the 1981 and 2008 and 2010 sample sets. However, correlations between gridded SST and a chronology generated from only 1981 otoliths coincided with correlations between gridded SST and a chronology generated using only the 2008 and 2010 otoliths (Fig. S4 in the Supplement). Also, we did not find evidence that latitude affected growth rates across the sampling area of the 2008 and 2010 otoliths. These results, in combination with the fact that all chronology samples crossdated with one another, suggest that the 1981 samples spatially overlapped with the 2008 and 2010 samples and that long-term trends in the RCS chronology were due to environmental variability.

Fish chronologies as developed here represent population-wide anomalies in otolith growth-increment widths, with likely relevance to somatic growth. For example, population-level anomalies in the length–weight relationship of YFS positively corresponded to the mean of the prior 3 or 4 values of

the otolith growth-increment chronology (Black et al. 2013). In other words, whether fish are, on average, relatively heavy or light at a given time appears to be a function of the otolith growth anomaly (the chronology) observed over the preceding few years. Such relationships between body condition and chronology have not been investigated for POP, although farther south in the California Current, levels of visceral fat in female yellowtail rockfish *S. flavidus* significantly decreased during the severe 1983 El Niño event (Lenarz & Echeverria 1986). The same year was characterized by low ecosystem productivity and a marked reduction in otolith growth across a range of rockfish species (Woodbury 1999, Black et al. 2011, Garcia-Reyes et al. 2013). It should be noted though that the chronologies developed here are relevant only to adult growth. The innermost otolith increments could also be measured and chronologies developed to establish long-term growth patterns and associated climate drivers for the first few years of life (Boehlert et al. 1989), but this would require fewer measurements per individual across a much larger number of exactly dated otoliths.

4.2. Climate–growth relationships and synchrony among species

The POP chronology positively correlated with MEI, PDO, and SST, as expected given that positive anomalies of all 3 indicators are associated with warm conditions in the North Pacific and Bering Sea. The El Niño-Southern Oscillation (ENSO) is teleconnected to the Aleutian Low, and is therefore evident in the oceanography and biology of the Bering Sea (Niebauer 1988, Rodionov et al. 2007). The PDO has also been widely documented to influence North Pacific ecosystem functioning and productivity (Francis et al. 1998, Hare & Mantua 2000), and can be defined as a 'reddened' response to ENSO forcing. Indeed, PDO at time t can be skillfully predicted by the PDO at $t - 1$ and the current ENSO (Newman et al. 2003, Shakun & Shaman 2009). Thus, as other studies have documented, biology is a function of remote and local environmental forcing.

The positive correlation between the POP chronology and SST could be due to direct effects of temperature on fish physiology. Indeed, rates of metabolism, consumption, and somatic growth are to some degree directly and generally positively affected by temperature (e.g. Brandt et al. 1992). An alternative explanation is that temperature created indirect effects via food supply. This is particularly evident in the California Current ecosystem where coastal upwelling lifts deep, cold, nutrient-rich water into the photic zone and thereby enriches primary production. There, rockfish otolith chronologies negatively correlate to temperature, as do other upper-trophic indicators of production, including seabird reproductive success (Black et al. 2008, 2011, Thompson & Hannah 2010).

In the Bering Sea, positive relationships between growth and temperature complicate efforts to disentangle whether environmental limitations are direct, indirect, or some combination thereof. However, consistently strong relationships with temperature for all available Bering Sea chronologies, including POP, YFS, Alaska plaice *Pleuronectes quadrituberculatus*, and northern rock sole *Lepidopsetta polyxystra*, may provide some indication (Matta et al. 2010, 2016, Black et al. 2013). If food supply is limiting, then the chronologies should track, at least in part, prey abundance or quality. If these prey are short-lived (<1 yr), then their abundance, and thus the predator chronology, should have strong high-frequency (interannual) signals and closely track climate drivers (Hsieh & Ohman 2006). In contrast, longer-lived prey species should dampen or 'integrate' climate drivers to a level that increases with longevity (Di Lorenzo & Ohman 2013). The diets of POP and YFS span a considerable range of species; for example, YFS primarily feeds on benthic and epibenthic invertebrates, whereas POP consumes prey higher in the water column, such as euphausiids, copepods, mysids, amphipods, and midwater fishes (Leaman 2002, Aydin et al. 2007). If food is limiting growth rates and if prey items live >1 yr, a chronology should likely have higher autocorrelation than climate indices. This was not found for YFS, for which no significant first-order autocorrelation was detected, and summer bottom temperatures alone explained >80% of the variation in the chronology (Black et al. 2013). Such close coupling with climate suggests the chronology could reflect direct effects of temperature, perhaps through effects on growing season length or metabolic activity. In contrast, the POP chronology had a higher level of autocorrelation ($r = 0.608$) than SST data from region 1 in Fig. 1 ($r = 0.482$; interval used 1969–2006), suggesting that food availability (i.e. indirect climate effects) might affect fish growth, at least partially. However, as only SSTs were available, and POP is generally found in deep water, there is the possibility that water at depth is more buffered to high-frequency variability, and that autocorrelation in POP was due to such a physical phenomenon.

Despite different life histories, habitats, and diets, there was synchrony between the POP and YFS

chronologies (Fig. 5). The most pronounced differences between these 2 chronologies were in the low-frequency domains. Compared with POP, the post-1976–1977 growth response of YFS was much more modest. YFS also experienced a conspicuous growth pulse in the early 2000s that was not shared by POP. Thus, low-frequency events were not necessarily synchronous across these Bering Sea shelf and slope species. The unusually long history provided by the POP chronology does suggest that for this species, the 1976–1977 regime shift was the most significant low-frequency event over the course of the 20th century, even compared with other North Pacific regime shifts in the early 1920s and mid-1940s (e.g. Mantua et al. 1997, Minobe 1997, Zhang et al. 1997), and more recently in 1989 (Hare & Mantua 2000, Bjorkstedt et al. 2011). Such a result is consistent with reports of a progressive 'reddening' of North Pacific climate in which fluctuations in the PDO have slowed over the course of the last century (Boulton & Lenton 2015). From a biological perspective, an ecosystem is more likely to track lower-frequency changes (Steele & Henderson 1994), which could at least partially explain the strong response of POP to the 1976–1977 regime shift. The POP chronology also indicates that growth increased over the course of the 20th century, which is consistent with long-term warming that has occurred in the region. The trend in POP has not been linear, however, following a step function, pre- versus post-1977. Ultimately, these chronologies underscore the susceptibility of fish biology to extreme low-frequency events, with responses that are not synchronous across species and sites.

Acknowledgments. We thank the crews of the FV 'Ryoan Maru No. 31' and FV 'Vesteraalen' for specimen collections and Chris Larsen and Chris Gburski (Alaska Fisheries Science Center) for help with otolith sectioning. We thank the participants of the North American Dendroecological Fieldweek (NADEF) for initial analysis of the samples, and Paul Spencer and Craig Kastelle from the Alaska Fisheries Science Center and 2 anonymous reviewers for their useful comments on an earlier version of the manuscript. The findings and conclusions in the paper are those of the authors and do not necessarily represent the views of the National Marine Fisheries Service. Reference to trade names does not imply endorsement by the National Marine Fisheries Service, NOAA.

LITERATURE CITED

Anderson PJ, Piatt JF (1999) Community reorganization in the Gulf of Alaska following ocean climate regime shift. Mar Ecol Prog Ser 189:117–123

Aydin K, Gaichas S, Ortiz I, Kinzey D, Friday N (2007) A comparison of the Bering Sea, Gulf of Alaska, and Aleutian Islands large marine ecosystems through food web modeling. NOAA Technical Memo NMFS-AFSC-178, US Department of Commerce, Seattle, WA

Bjorkstedt EP, Goericke R, McClatchie S, Weber E and others (2011) State of the California Current 2010–2011: regionally variable responses to a strong (but fleeting?) La Niña. CCOFI Rep 52:36–68

Black BA (2009) Climate driven synchrony across tree, bivalve, and rockfish growth-increment chronologies of the northeast Pacific. Mar Ecol Prog Ser 378:37–46

Black BA, Boehlert GW, Yoklavich MM (2005) Using tree-ring crossdating techniques to validate annual growth increments in long-lived fishes. Can J Fish Aquat Sci 62: 2277–2284

Black BA, Gillespie D, MacLellan SE, Hand CM (2008) Establishing highly accurate production-age data using the tree-ring technique of crossdating: a case study for Pacific geoduck (*Panopea abrupta*). Can J Fish Aquat Sci 65:2572–2578

Black BA, Schroeder ID, Sydeman WJ, Bograd SJ, Wells BK, Schwing FB (2011) Winter and summer upwelling modes and their biological importance in the California Current Ecosystem. Glob Change Biol 17:2536–2545

Black BA, Matta ME, Helser TE, Wilderbuer TK (2013) Otolith biochronologies as multidecadal indicators of body size anomalies in yellowfin sole (*Limanda aspera*). Fish Oceanogr 22:523–532

Black BA, Sydeman WJ, Frank DC, Griffin D and others (2014) Six centuries of variability and extremes in a coupled marine-terrestrial ecosystem. Science 345:1498–1502

Boehlert GW, Yoklavich MM, Chelton DB (1989) Time series of growth in the genus *Sebastes* from the northeast Pacific Ocean. Fish Bull 87:791–806

Boulton CA, Lenton TM (2015) Slowing down of North Pacific climate variability and its implications for abrupt ecosystem change. Proc Natl Acad Sci USA 112: 11496–11501

Brandt SB, Mason DM, Patrick EV (1992) Spatially-explicit models of fish growth rate. Fisheries (Bethesda, MD) 17: 23–33

Briffa KR, Jones PD (1990) Basic chronology statistics and assessment. In: Cook ER, Kairiukstis LA (eds) Methods of dendrochronology. Kluwer Academic Publishers, Dordrecht, p 137–152

Cavalieri D, Parkinson C, Gloersen P, Zwally HJ (1996) Sea ice concentrations from Nimbus-7 SMMR and DMSP SSM/I-SSMIS. I. Passive microwave data. National Snow and Ice Data Center, Boulder, CO, updated yearly. http://nsidc.org/data/NSIDC-0051/versions/1 (accessed Jan 2016)

Conners ME, Hollowed AB, Brown E (2002) Retrospective analysis of Bering Sea bottom trawl surveys: regime shift and ecosystem reorganization. Prog Oceanogr 55: 209–222

Cook ER, Briffa KR, Meko DM, Graybill DA, Funkhouser G (1995) The 'segment length curse' in long tree-ring chronology development for palaeoclimatic studies. Holocene 5:229–237

Di Lorenzo E, Ohman MD (2013) A double-integration hypothesis to explain ocean ecosystem response to climate forcing. Proc Natl Acad Sci USA 110:2496–2499

Douglass AE (1936) Climatic cycles and tree-growth, Vol III. Carnegie Institution, Washington, DC

Esper J, Cook ER, Schweingruber FH (2002) Low-frequency

signals in long tree-ring chronologies for reconstructing past temperature variability. Science 295:2250–2253

Esper J, Cook ER, Krusic PJ, Peters K, Schweingruber FH (2003) Tests of the RCS method for preserving low-frequency variability in long tree-ring chronologies. Tree-Ring Res 59:81–98

Francis RC, Hare SR, Hollowed AB, Wooster WS (1998) Effects of interdecadal climate variability on the oceanic ecosystems of the NE Pacific. Fish Oceanogr 7:1–21

Fritts HC (1976) Tree rings and climate. Academic Press, New York, NY

Garcia-Reyes M, Sydeman WJ, Thompson SA, Black BA, Rykaczewski RR, Thayer JA, Bograd SJ (2013) Integrated assessment of wind effects on central California's pelagic ecosystem. Ecosystems 16:722–735

Goetz BJ, Piston CE, Gburski CM (2012) Rockfish (*Sebastes*) species. In: Matta ME, Kimura DK (eds) Age determination manual of the Alaska Fisheries Science Center Age and Growth Program. NOAA Professional Paper 13, US Department of Commerce, Seattle, WA

Grissino-Mayer HD (2001) Evaluating crossdating accuracy: a manual and tutorial for the computer program COFECHA. Tree-Ring Res 57:205–221

Hare SR, Francis RC (1995) Climate change and salmon production in the Northeast Pacific Ocean. In: Beamish RJ (ed) Climate change and northern fish populations. Canadian Special Publication of Fisheries and Aquatic Sciences 121, Department of Fisheries and Oceans, Ottawa

Hare SR, Mantua NJ (2000) Empirical evidence for North Pacific regime shifts in 1977 and 1989. Prog Oceanogr 47: 103–145

Hollowed AB, Wooster WS (1995) Decadal-scale variation in the eastern subarctic Pacific: II. Response of Northeast Pacific fish stocks. In: Beamish RJ (ed) Climate change and northern fish populations. Canadian Special Publication of Fisheries and Aquatic Sciences 121, Department of Fisheries and Oceans, Ottawa

Holmes RL (1983) Computer-assisted quality control in tree-ring dating and measurement. Tree-Ring Bull 43:69–78

Hsieh CH, Ohman MD (2006) Biological responses to environmental forcing: the linear tracking window hypothesis. Ecology 87:1932–1938

Hunt Jr. GL, Stabeno P, Walters G, Sinclair E, Brodeur RD, Napp JM, Bond NA (2002) Climate change and control of the southeastern Bering Sea pelagic ecosystem. Deep-Sea Res II 49:5821–5853

Hunt Jr. GL, Coyle KO, Eisner LB, Farley EV and others (2011) Climate impacts on eastern Bering Sea foodwebs: a synthesis of new data and an assessment of the oscillating control hypothesis. ICES J Mar Sci 68:1230–1243

Kastelle CR, Kimura DK, Goetz BJ (2008) Bomb radiocarbon age validation of Pacific ocean perch (*Sebastes alutus*) using new statistical methods. Can J Fish Aquat Sci 65: 1101–1112

Leaman B (2002) *Sebastes alutus*. In: Love MS, Yoklavich M, Thorsteinson L (eds) The rockfishes of the Northeast Pacific. University of California Press, Berkeley

Lenarz WH, Echeverria TW (1986) Comparison of visceral fat and gonadal fat volumes of yellowtail rockfish, *Sebastes flavidus*, during a normal year and a year of El Niño conditions. Fish Bull 84:743–745

Litzow MA, Mueter FJ, Hobday AJ (2014) Reassessing regime shifts in the North Pacific: incremental climate change and commercial fishing are necessary for explaining decadal-scale biological variability. Glob Change Biol 20:38–50

Mantua NJ, Hare SR, Zhang Y, Wallace JM, Francis RC (1997) A Pacific interdecadal climate oscillation with impacts on salmon production. Bull Am Meteorol Soc 78: 1069–1079

Matta ME, Black BA, Wilderbuer TK (2010) Climate-driven synchrony in otolith growth-increment chronologies for three Bering Sea flatfish species. Mar Ecol Prog Ser 413: 137–145

Matta ME, Helser TE, Black BA (2016) Otolith biochronologies reveal latitudinal differences in growth of Bering Sea yellowfin sole *Limanda aspera*. Polar Biol, doi: 10.1007/s00300-016-1917-y

Minobe S (1997) A 50–70 year climatic oscillation over the North Pacific and North America. Geophys Res Lett 24: 683–686

Newman M, Compo GP, Alexander MA (2003) ENSO-forced variability of the Pacific decadal oscillation. J Clim 16: 3853–3857

Niebauer HJ (1988) Effects of El Niño–Southern Oscillation and North Pacific weather patterns on interannual variability in the subarctic Bering Sea. J Geophys Res, C, Oceans 93:5051–5068

Poloczanska ES, Brown CJ, Sydeman WJ, Kiessling W and others (2013) Global imprint of climate change on marine life. Nat Clim Change 3:919–925

Pörtner HO, Karl DM, Boyd PW, Cheung WWL and others (2014) Ocean systems. In: Field CB, Barros VR, Dokken DJ, Mach KJ and others (eds) Climate change 2014: impacts, adaptation, and vulnerability. A. Global and sectoral aspects. Contribution of Working Group II to the Fifth Assessment Report of the Intergovernmental Panel on Climate Change. Cambridge University Press, Cambridge

Rayner NA, Parker DE, Horton EB, Folland CK and others (2003) Global analyses of sea surface temperature, sea ice, and night marine air temperature since the late nineteenth century. J Geophys Res, D, Atmospheres 108:4407

Rodionov SN (2004) A sequential algorithm for testing climate regime shifts. Geophys Res Lett 31:L09204

Rodionov SN (2006) Use of prewhitening in climate regime shift detection. Geophys Res Lett 33:L12707

Rodionov SN, Bond NA, Overland JE (2007) The Aleutian Low, storm tracks, and winter climate variability in the Bering Sea. Deep-Sea Res II 54:2560–2577

Shakun JD, Shaman J (2009) Tropical origins of North and South Pacific decadal variability. Geophys Res Lett 36: L19711

Stabeno PJ, Kachel NB, Moore SE, Napp JM, Sigler M, Yamaguchi A, Zerbini AN (2012) Comparison of warm and cold years on the southeastern Bering Sea shelf and some implications for the ecosystem. Deep-Sea Res II 65–70:31–45

Steele JH, Henderson EW (1994) Coupling between physical and biological scales. Philos Trans R Soc Lond B Biol Sci 343:5–9

Thompson JE, Hannah RW (2010) Using cross-dating techniques to validate ages of aurora rockfish (*Sebastes aurora*): estimates of age, growth and female maturity. Environ Biol Fishes 88:377–388

Trouet V, Van Oldenborgh GJ (2013) KNMI Climate

Explorer: a web-based research tool for high-resolution paleoclimatology. Tree-Ring Res 69:3–13

Walsh JJ, McRoy CP (1986) Ecosystem analysis in the southeastern Bering Sea. Cont Shelf Res 5:259–288

Wang MY, Overland JE, Stabeno P (2012) Future climate of the Bering and Chukchi seas projected by global climate models. Deep-Sea Res II 65–70:46–57

Wigley TML, Briffa KR, Jones PD (1984) On the average value of correlated time-series, with applications in dendroclimatology and hydrometeorology. J Clim Appl Meteorol 23:201–213

Wolter K, Timlin MS (2011) El Niño/Southern Oscillation behaviour since 1871 as diagnosed in an extended multivariate ENSO index (MEI.ext). Int J Climatol 31: 1074–1087

Woodbury D (1999) Reduction of growth in otoliths of widow and yellowtail rockfish (*Sebastes entomelas* and *S. flavidus*) during the 1983 El Nino. Fish Bull 97:680–689

Zhang Y, Wallace JM, Battisti DS (1997) ENSO-like interdecadal variability: 1900–93. J Clim 10:1004–1020

Editorial responsibility: Nils Chr. Stenseth, Oslo, Norway

Submitted: June 1, 2016; Accepted: August 18, 2016
Proofs received from author(s): November 7, 2016